Peierls or Jahn-Teller effect in endohedrally doped silicon clathrates: An EXAFS study

F. Brunet, P. Mélinon, A. San Miguel, P. Kéghélian, and A. Perez
Département de Physique des Matériaux, Université Claude Bernard-Lyon 1, F 69622 Villeurbanne, France

A. M. Flank
LURE Centre Universitaire Paris Sud, Batiment 209D, Bôite Postal 34, F 91898 Orsay, Cedex, France

E. Reny, C. Cros, and M. Pouchard
Institut de Chimie de la Matière Condensée de Bordeaux, Université de Bordeaux I, 33608 Pessac, France
(Received 6 October 1999; revised manuscript received 8 February 2000)

The effect of doping silicon clathrate structures with sodium atoms has been investigated experimentally by x-ray photoemission and x-ray absorption spectroscopies. Both techniques reveal a poor screening of the sodium atoms inside the silicon cages. We also discuss the sodium state that is intermediate between the metal-like and the atomlike ones. These results are in agreement with theoretical predictions of Demkov *et al.* and Smelyansky and Tse. In addition, the fine analysis of the extended x-ray absorption fine structure region reveals unambiguously a large displacement (0.9 ± 0.2 Å) of the sodium atom with respect to the center of the silicon cage. This displacement is higher than the one predicted by a simple Jahn-Teller effect and is discussed in terms of sodium pairing. The formation of dimers with covalent bonding is compared to the Peierls distortion in a monodimensional network.

I. INTRODUCTION

Covalent cagelike assembled crystals have been studied both experimentally[1–18] and theoretically.[19–32] These structures form large polyhedral cavities that can accommodate templating guest species allowing a wide variety of novel compounds. A well-known example is common C_{60} pristine: a fcc arrangement of C_{60} fullerenes.[1] Owing to the particular hybridization in C_{60}, the cages are weakly bound by van der Waals interaction and pristine and keep a large memory of the C_{60} molecular character.[32,33] In silicon or germanium clathrates, the building block polyhedra share their faces leading to a rigid lattice. In these clathrates, atoms are fourfold coordinated just as they are in the diamond phase. While, in pristine the pentagons (*i.e., carbon fivefold rings*) are isolated, clathrates are formed by fullerenes having isolated hexagons, and consequently fused pentagons. This is required since fused hexagons introduce a significant π bonding as in graphene that is not energetically favorable in silicon and germanium. Among the huge fullerene family, four polyhedra (namely, Si_{20}, Si_{24}, Si_{26}, and Si_{28}) are potential candidates to form an infinite periodic lattice by combining together.[8] In fact, two clathrates are commonly observed labeled Si-46 and Si-34. The Si-46 is formed by a simple cubic arrangement of Si_{20} and Si_{24} polyhedra, while Si-34 is formed by a fcc arrangement of Si_{20} and Si_{28} polyhedra. The Si-34 lattice structure is analogous to the common diamond where each Si atom has been replaced by a Si_{28} polyhedron. Both pristine and clathrate exhibit superconductivity when selected additional atoms are placed between the cages or within the cages.[11,3,4] It is admitted that the conventional-mediated Bardeen-Cooper-Schreffer mechanisms could explain the observed superconductivity. In addition, a connection between Jahn-Teller distortion energies and high-T_c superconductivity has been emphasized.[34,35] Since the McMillan equation for T_c (Ref. 36) reveals that high T_c is promoted by a high Debye frequency, superconductivity is favored in carbon-cage assembled materials with respect to silicon ones. In addition, the Jahn-Teller distortion is enhanced in small clusters having a sp^3 hybridization (such as in clathrate).[36] Thus, carbon clathrates could be interesting candidates for new high-T_c superconductors. Unfortunately, such structures, which are probably stable, to our knowledge, have not been yet reported. In this paper, we report the observation of a Peierls-Jahn-Teller distortion in Na_8@Si-34 from a careful analysis of the EXAFS region (extended x-ray absorption fine structure) at the Na *K* edge. In addition, the XANES (x-ray absorption near-edge structure) region analysis and additional x-ray photoemission spectroscopy (XPS) measurements reveal the absence of an ionic state for the alkali in agreement with other results. The semi-metal-like state is corroborated by the poor screening of the photoelectron observed in XPS and XANES. In addition, the measurement of the Fermi level position with respect to the valence-band minimum is in agreement with theoretical results.

II. CLATHRATE: JAHN-TELLER EFFECT AND CONDUCTION MECHANISMS

Figure 1 shows the Si-34 and Na_8@Si-34 lattices. The whole symmetry of the crystal is $Fd\bar{3}m$ as in diamond, Si-2. Isolated Si_{20} and Si_{28} polyhedra, which form the Si-34 lattice, have the I_h and T_d point symmetry, respectively. It has been established that both types of polyhedron are unstable owing to a large Jahn-Teller interaction.[36] In a weak electron correlation picture T_d Si_{28} has a degenerate electronic eigenstate at the Fermi level (a triplet occupied by only four electrons). This and the presence of an empty singlet state lying a few tenths of eV above the triplet suggests that the Si_{28}

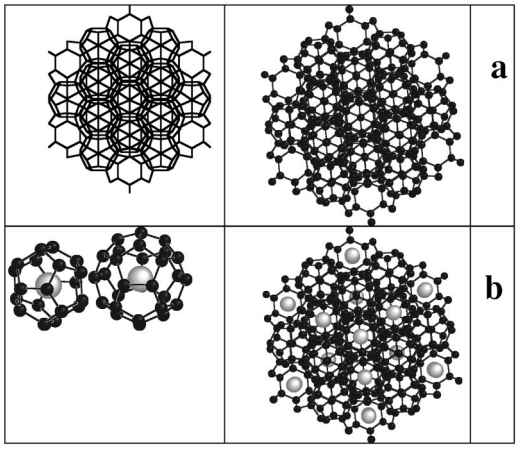

FIG. 1. Si-34 clathrate projected along the [111] direction. (a) The structure skeleton with visible cages is shown (left panel). The empty clathrate is shown (a) (right panel) with the silicon atoms in dark color. (b) (right panel) shown is the Na_8@Si-34 structure with the sodium atoms in gray color. The left panel of (b) shows the two elemental cells forming the clathrate: Na@Si_{20} and Na@Si_{28}. In Na_8@Si-34, the Si_{20} cages are empty. (Na atoms have been placed at the center of the cages.)

cage can be viewed as a closed-shell structure with a large gap if each atom adopts a $4\bar{3}m$ conformation as in clathrates. Likewise, in the same scheme, Si_{20} has an open shell with a fourfold degenerated HOMO occupied by two electrons. Thus, the equilibrium geometry of this molecule cannot be icosahedral. In the lattice, the geometry of both polyhedra is slightly deformed. In order to characterize the distortion of the polyhedron, we have calculated from our experimental x-ray powder diffraction (XRD) the coordinance shells from the center of either polyhedron (Table I). These parameters will be used as input for the interpretation of the EXAFS measurements as discussed below. In Na_8@Si-34 each hexakaidecahedron is fully occupied by one sodium atom. Owing to the whole lattice symmetry, the sodium network forms a giant diamond lattice where each sodium atom has four sodium neighbors ($d_{Na-Na}=6.34$ Å) (Fig. 2). This particular sodium concentration corresponds to the expected insulator-to-metalliclike transition experimentally observed by different techniques. In fact, an insulator-to-metal transition is observed in Na_x@Si-34 clathrates compounds when the guest atom concentration increases significantly ($x>8$). The transition mechanism is still debated owing to the weak interaction between sodium and silicon. First-principles calculations rule out the hypothesis of a degenerated semiconductor where electrons could be thermally excited into the conduction band.[31] Smelyansky and Tse have found that the bottom

TABLE I. Selected crystallographic data for Na_8@Si-34 and distances between the center of the cage (labeled X) and the silicon shells d_{Na-Si} belonging to both polyhedra Si_{20} and Si_{28}, respectively (right panel). The left panel gives the average distance assuming perfect I_h and T_d structures for Si_{20} and Si_{28}, respectively.

Name notation	Clathrate Na_8@Si-34
Space group Lattice constant	$Fd\bar{3}m$ origin at center $\bar{3}m$ 14.65 Å
Position	(x,y,z) $(\mathrm{Si})(x,x,x), x=1/8$ $(\mathrm{Si})(x,x,x), x=0.781$ $(\mathrm{Si})(x,x,z), x=0.817; z=0.629$ $(\mathrm{Na})(x,x,x), x=3/8$ $(\mathrm{Na})(x,x,x), x=0$ (in Na_{24}@Si-34)
Expected free Si_{28} without Jahn-Teller distortion	Si_{28} in the Si-34 clathrate
$d_{X\text{-Si}}=3.95$ Å, $N=28$	$d_{X\text{-Si}}=3.91$ Å, $N=12$ $d_{X\text{-Si}}=3.96$ Å, $N=4$ $d_{X\text{-Si}}=3.98$ Å, $N=12$ mean deviation 0.03 Å
Expected free Si_{20} without Jahn-Teller distortion	Si_{20} in the Si-34 clathrate
$d_{X\text{-Si}}=3.31$ Å, $N=20$	$d_{X\text{-Si}}=3.17$ Å, $N=2$ $d_{X\text{-Si}}=3.27$ Å, $N=6$ $d_{X\text{-Si}}=3.36$ Å, $N=12$ mean deviation 0.05 Å

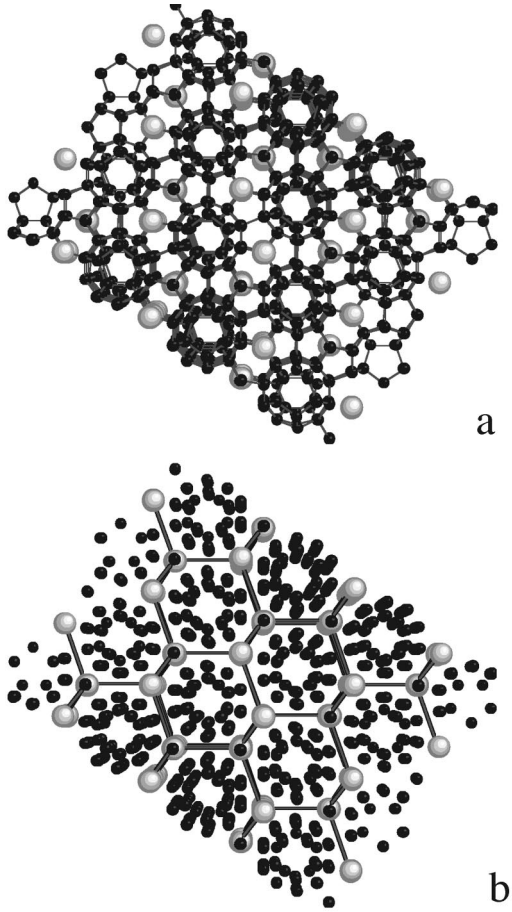

FIG. 2. Na_8@Si-34 lattice. (a) The lattice with all silicon atoms bounded; (b) the same lattice with all the sodium atoms bound. The sodium lattice forms a giant diamond lattice with $d_{Na\text{-}Na}=6.43$ Å. (Na atoms have been placed at the center of the cages.)

of the conduction band is flat and mainly occupied by the Na 3*s* density of states. This band is empty, half occupied, and fully occupied in Si-34, Na_4@Si-34, and Na_8@Si-34, respectively. Due to its symmetry, this band is threefold degenerated at Γ point. Consequently, it is expected that a Jahn-Teller effect lifts this degeneracy.[37] Using quantum molecular dynamics associated to a modified tight binding scheme, Demkov *et al.*[37] have studied this Jahn-Teller effect. They found in Na_4@Si-34 a splitting between the levels at Γ point of 0.065 eV. Thus, the Na_8@Si-34 is, in a simple scheme, an insulator since the bottom of the conduction band remains fully occupied. In addition, Smelyansky and Tse[31] have observed that the band located just above the conduction-band minimum (CBM) at Γ point (without taking into account the Jahn-Teller splitting) shifts lower in energy as the sodium concentration increases (Na_x@Si-34, $0<x<8$). Finally, the separation between this band and the CBM is estimated at 0.06 eV, which is of the same order of magnitude as the expected Jahn-Teller gap. The conduction mechanism in Na_8@Si-34 is still debated. While Demkov *et al.*[37] suggest a correlation-induced metal, where electrons are excited over the Jahn-Teller gap, Smelyansky and Tse[31] argue that the concave curvature of the levels lying at the bottom of the conduction bands explains the poor conductivity owing to the weak density of states near the Fermi level.

III. EXPERIMENTAL PROCEDURE

We have used the same Na_8@Si-34 clathrate samples for all experiments, i.e., XRD, inelastic neutron scattering,[16] XPS, XANES, and EXAFS. The last three will be reported here. The samples are powders with a mean grain size of the order of a few micrometers and were obtained by thermal decomposition of NaSi under vacuum (10^{-6} Torr) in the temperature range 670–710 K. We are not able to produce pure Si-34 and we have used a sample containing a poor concentration of sodium (Na_x@Si-34, $x<1$) as a template of pure Si-34. This concentration is not enough to affect significantly the region close to the conduction-band minimum.

The powder (300 mesh) is mounted on gallium or indium substrates in order to minimize the charge space effect during XPS, Auger, or x-ray absorption spectroscopies (XAS). The powder is shared out of the substrate in order to get a continuous thin film. The samples are chemically etched by immersion in HF solution and blown dry with nitrogen prior their introduction in the XPS or XAS devices. This procedure is essential to removing any Si-O bond located at the surface of the grains.

The spectrometer is a dual XPS/Auger camera Nanoscan-100-type microprobe operating at a base pressure less than 4×10^{-10} Torr. The sample area analyzed in XPS mode is about a few mm^2. The XPS is performed using an Al $K\alpha$ x-ray (1486.6 eV). The resolution was fixed at 1 eV for the core level. Clathrate samples are compared to a nearly intrinsic Si (100) crystal ($\rho>400\ \Omega$ cm *n*-type at room temperature, labeled ''Si-2'') or to fine silicon powder (99 999% purity).

Si *K*-edge absorption spectra of crystalline Na_1@Si-34, Na_8@Si-34, and Si-2 were recorded collecting the total drain current and/or the fluorescence emission as a function of the photon energy. The measurements were performed on a beam line SA32 (located at the 800-MeV positron storage ring SuperACO in Orsay, France). The x-ray beam was monochromatized by an InSb (111) double-crystal monochromator (0.7 eV resolution). Several scans were collected to ensure the true estimation of the systematic errors in the parameters to be determined. Energy calibration was done using the absorption edge at 1839 eV for Si-2. All samples were analyzed using the same standard procedure. Some aspects of the XANES and EXAFS regions at the Si *K* edge will be discussed here. More details will be given in a forthcoming paper.[38]

Na *K*-edge absorption spectra of Na_8@Si-34 have been recorded at three temperatures 20 K, 100 K, and 300 K in the fluorescence mode. The x-ray beam was monochromatized by a $(10\bar{1}0)$ beryls double-crystal monochromator (0.4 eV resolution). A low-temperature measurement is useful since the Na-Si coupling factor is weak and the Debye-Waller contribution is expected to be large. For example, in Na_8@Si-34 we have found a vibrational Einstein-like mode located at 6.6 meV leading to an Einstein temperature of around 76 K.[16] Since the sodium atom is located into a nearly spherical sphere of Si atoms, its mean position into the polyhedron depends on the mean-vibrational amplitude $\langle u_x^2\rangle$. Consequently, its true position is better determined as far as the lattice temperature is lower than the Einstein temperature.

Si_{1s} and Na_{1s} core level lines have been deduced from the derivative of the Si and Na *K*-edge absorption in XAS experiment, respectively. The general principle of Si or Na *K*-edge absorption spectroscopy is to excite the occupied core shell Si_{1s} or Na_{1s} electron towards the empty conduction band. In intrinsic semiconductors, XAS spectroscopy probes the core level line related to the conduction band minimum (CBM). This is expected to be true for Si-2 and Na_1@Si-34 since both are insulators. Following theoretical predictions,[31,37] the Fermi level in Na_8@Si-34 is pulled up in the conduction band, and the core level line will be rather related to the Fermi level. It is worthwhile to compare our data with other sodium states (atom, free ion, etc.) in order to characterize the electronic state. For this purpose, we have to estimate the difference between the Fermi level and/or the CBM and the vacuum level. In Si-2, this difference just coincides with the electron affinity (4 eV). For clathrate, this is more complicated. In a previous paper,[15] we have mentioned a band-gap opening in the clathrate (1.9 eV and 1.2 eV for Si-34 and Si-2, respectively). According to the effective mass theory where the CBM shift is on the same order of magnitude as the valence-band maximum (VBM) shift,[41] we can expect a decrease of the electron affinity in the clathrate. Its value will be close to $(4-0.7/2)=3.65$ eV. Such a value will be used for scaling the core level line to the vacuum level. Since XAS spectroscopy probes the core level related to the CBM, the binding energy to the vacuum level of Na_{1s} in NaCl is obtained just adding the electron affinity of the NaCl crystal (0.9 eV) to our experimental data.

Na_{1s} core level line has been deduced from both XAS and XPS spectra. For XAS spectra, the scaling of the core level line related to the vacuum level will be discussed later. In XPS spectroscopy, the core level line is related to the Fermi level. We follow Siegbahn *et al.*[40] and assume that in the XPS device, the difference between the Fermi level and the vacuum level is given by the work function (4 eV typically). The choice of the reference level is less clear owing to the unknown contact potentials and especially the nature of the Schottky barrier.

IV. XANES/XPS SPECTROSCOPIES

A. Fermi level position and Si_{1s} core level line

Figure 3(a) shows the Si *K*-edge normalized XAS spectra of Na_1@Si-34, Na_8@Si-34, and Si-2, respectively. We have measured the Si-2 reference samples (single crystal or powder) just before and after the measurement of the clathrate ones, allowing the correction of a possible energy drift during the experiment. Nevertheless, no significant shift has been found within our precision (less than 0.1 eV). The presence of SiO_2 contamination can be excluded from the absence of any significant contribution located at 1847 eV. The resonance (labeled a) located near 1843 eV appears in all samples, while the one (labeled c) located near 1852 eV in Na_1@Si-34 and Si-2 is shifted (labeled d) towards high energy in Na_8@Si-34. This resonance is comparable in Na_1@Si-34 and the diamond phase and is attributed to simple/multiple scattering effects in the intermediate XANES/EXAFS region.[38] Figure 3(b) shows the derivative of the absorption threshold in these samples. Na_1@Si-34 and Na_8@Si-34 core level lines are slightly shifted towards low

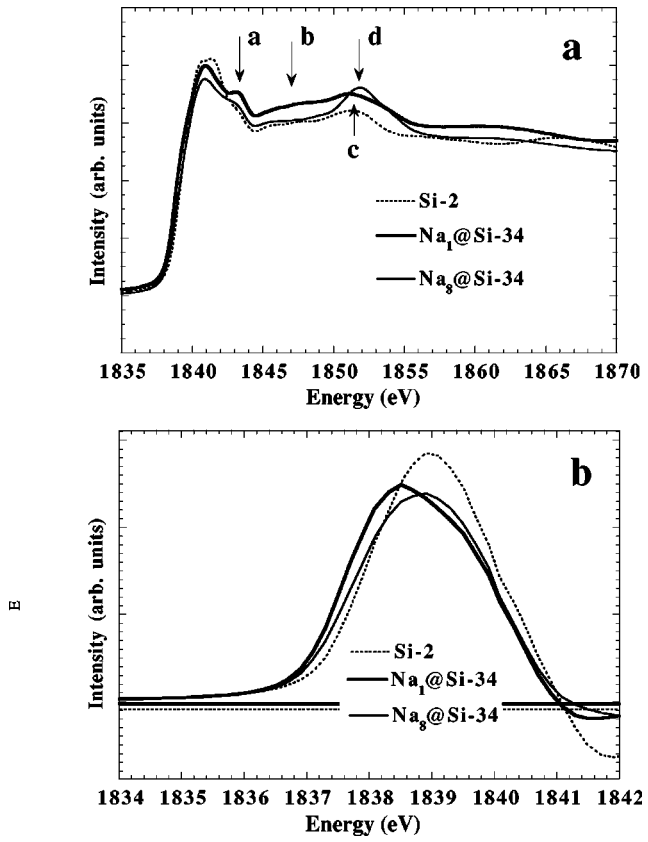

FIG. 3. (a) Si *K*-edge x-ray absorption spectra (XANES region) for various silicon samples. (a),(c),(d) identify different resonances. (b) The Si_{1s} core level line in Si-O bond. (b) The core line obtained from the derivative of curves in panel (a) around the edge energy. In this case, the energy is related to the vacuum level (see text).

energy with respect to Si-2. Since Na_8@Si-34 core level line is shifted by about 0.25 ± 0.1 eV with respect to Na_1@Si-34, we expect that the Fermi level in Na_8@Si-34 lies at 0.25 eV above the CBM. This value is not so far from the absolute precision of our device. It is still well reproducible and seems accurate. Finally, the corrected values related to the vacuum level are $1839.0+4=1843.0$ eV and $1838.6+3.65=1842.25\pm0.2$ eV for Si-2 and Si-34, respectively.

B. Sodium state

Figures 4(a) and 4(b) show the Na_{1s} core level lines in NaCl and Na_8@Si-34 deduced from XAS spectroscopy. The energy is related to the vacuum level with the procedure mentioned above. For Na_8@Si-34, the raw position related to the Fermi level is corrected by adding the estimated electron affinity in the clathrate (3.65 eV) minus the separation between the Fermi level and the CBM (0.25 eV). Table II gives the position of the Na_{1s} core level lines in other sodium compounds for comparison. Figure 4(c) shows the Na_{1s} core level lines in NaCl and Na_8@Si-34 deduced from XPS spectroscopy. Both spectroscopies show a Na_{1s} core level state lying at higher energy than the one observed in NaCl (see Table II). The discrepancy between NaCl values in XAS and XPS can be attributed to the dubiousness of the Na_{1s} core level state position in XPS spectroscopy and absolute calibration in XAS.[39]

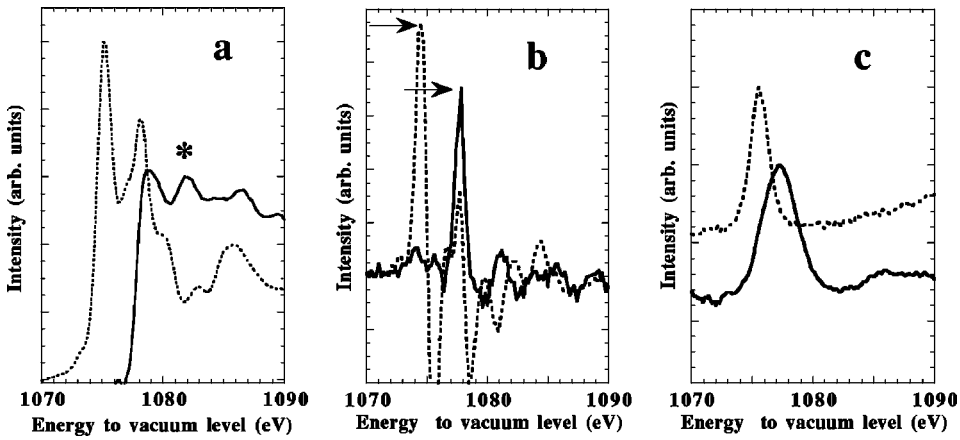

FIG. 4. (a) Sodium *K*-edge absorption spectra (XANES region) in NaCl (dashed line) and Na_8@Si-34 (full line) recorded collecting the total drain current. The shoulder marked by a star is interpreted as an artifact of the measurement: it has no physical interpretation and it is not observed on spectra recorded collecting the fluorescence intensity. (b) The core level lines obtained from the derivative of the curves (a). In this case, the energy is related to the vacuum level (see text). (c) The core level lines obtained by XPS spectroscopy.

V. EXAFS

A. Data analysis

Na *K*-edge x-ray absorption spectra of Na_8@Si-34 recorded at three temperatures 20 K, 100 K, and 300 K are reported in Fig. 5. In order to extract the EXAFS oscillation from the absorption spectra the atomic absorption was modeled by a third-order polynomial expression and the normalization was done using the Lengeler-Eisenberg algorithm. EXAFS oscillations were expressed in terms of the photoelectron wave number $k=(1/\hbar)\sqrt{2}m(E-E_0)$, where m is the electron mass and E_0 is chosen at the inflection point of the threshold.

Even though the crystallographical structure of pure silicon clathrate is perfectly known, ambiguities on the sodium position inside the Si_{28} polyhedra are still of actuality. Si_{28} polyhedra are composed of four hexagonal faces (tetragonal symmetry) and 12 pentagonal faces. In such a structure, we are able to accurately calculate the sodium-silicon bond length (R_i) and the coordination numbers (N_i) whatever the sodium position is in the Si_{28} polyhedra. Then we can compute single and multiple scattering paths contributing to the EXAFS signal and adjust some fitting parameters.

The contributions of single and multiple scattering paths to the EXAFS signal are calculated within the framework of *ab initio* self-consistent real space multiple-scattering FEFF code (FEFF8).[43] For this purpose, we take a cluster formed by a sodium atom surrounded by 99 silicon atoms and consider the most significant 160 single and multiscattering pathways. We have checked that the number of pathways is significative enough to reproduce the EXAFS signal. As a preliminary, we calculate the XAFS spectra without introducing the Debye temperature. The set of experimental data ($T=20$ K, 100 K, and 300 K) is then fitted using the FEFFIT code.[44] Mathematically, we have only three fitting variables to optimize $k^2\chi(k)$: the Debye temperature, the amplitude reduction factor S_0^2, and the E_0 threshold. In addition, these variables must be constrained through physical arguments.

(i) The E_0 threshold is expected to be the same for the three experimental spectra ($T=20$ K, 100 K, and 300 K).

(ii) XAFS spectra are referenced to the threshold Fermi level. This value is determined with the self-consistent field (SCF) procedure on a cluster of 86 atoms centered on the Na atom within a fraction of eV. Consequently, we have constrained the range of variation of E_0 in the fit to be between $+1$ eV and -1 eV. We have also calculated the XAFS spectra from the standard overlapped atom potentials where the precision is lower than in the case of a self-consistent calculation but for which the computing time is drastically reduced. The error in the position of the Fermi level is in that last case of about 3 eV.

(iii) S_0^2 is the same for all the experimental spectra and was arbitrarily set $S_0^2=1$. Remember that S_0^2 and the Debye temperature are strongly correlated and this arbitrary choice can have some incidence in the value of this last variable.

(iv) The sodium atom can be displaced away from the center of the cage towards the center of an hexagon where the electron density cloud is the smallest (i.e., we minimize the sodium-silicon overlapping). We note this displacement as ΔR.

(v) The Debye temperature is not well defined but can be estimated in a certain range. In an earlier paper, from neutron inelastic scattering performed in the same samples, we have

TABLE II. Na_{1s} core level line for different sodium states. The free ion state is from Ref. 45. Atomiclike and standard values in bulk phase (bcc) are from Ref. 47.

Na_{1s}	Na_{1s} bulk metal	Na_{1s} free ion	Na_{1s} in NaCl (our work)	Na_{1s} in Na_8@Si-34 (our work)
1079.1 eV	1074 eV	1088.2 eV	1074.4 eV (XAS) 1075.4 eV (XPS)	1077.8 eV (XAS) 1077.2 eV (XPS)

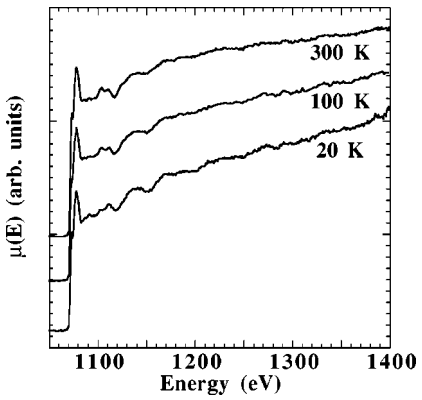

FIG. 5. Na *K*-edge x-ray absorption spectra of Na_8@Si-34 recorded at 20 K, 100 K, and 300 K.

found a localized vibrating mode corresponding to the coupling between the sodium atom and the silicon host ($\hbar\omega_{Na-Si}=6.6$ meV). This mode corresponds to a typical Einstein temperature $\theta_E=79$ K (using the Debye approximation $\theta_D=4/3\theta_E=106$ K). This value corresponds to the expected lower limit in our fit. On the contrary, we assume that the Debye frequency cannot exceed the one of the silicon host, which is not so far from the classical Si-2 $\theta_D=640$ K.

From the SCF calculation, we found a strong correlation between the E_0 threshold and ΔR. Since E_0 is constrained within the accuracy of the used model [see assumption (ii)], ΔR is also constrained in a certain range. Moreover, we found also a better fit (measured by χ^2) when E_0 is in the range $+1$ eV to -1 eV. Furthermore, the fit gave the same Debye temperature for all experimental spectra ($T=20$ K, 100 K, and 300 K). We emphasize that the physical robustness of this fit comforts us on the physical meaning of the sodium displacement. On the contrary, we are less confident on the physical meaning and accuracy of the Debye temperature, first because of the complexity of the geometry around the Na atom when displaced and second because of the strong coupling with S_0^2 and with the normalization procedure.

We now return to the assumption labeled (iv). In fact, other displacement directions of the sodium atom should not be, *a priori*, disregarded. However, a complete study of all the parameters needs a prohibitive computer time with regards to a self-consistent scattering potential calculation. Consequently, in some parts of our study, we have used the overlapped potential method, which needs a much reduced computer time. Even if both methods achieve a similar fit, the accuracy in ΔR is reduced in the last one and we cannot use a single Debye temperature at all measured temperatures. Nevertheless, a slight variation of the Debye temperature versus the experimental temperature could be interpreted as an artifact introduced by some partial anharmonicity and/or anisotropy in the sodium-silicon vibration motion.

B. Results

Figure 6 displays the raw EXAFS signal and the fit (panel 6a: fits using self-consistent scattering potential; panel 6b: fits using standard overlapped atom potentials) obtained at 20 K, 100 K, and 300 K, respectively. The displacement of

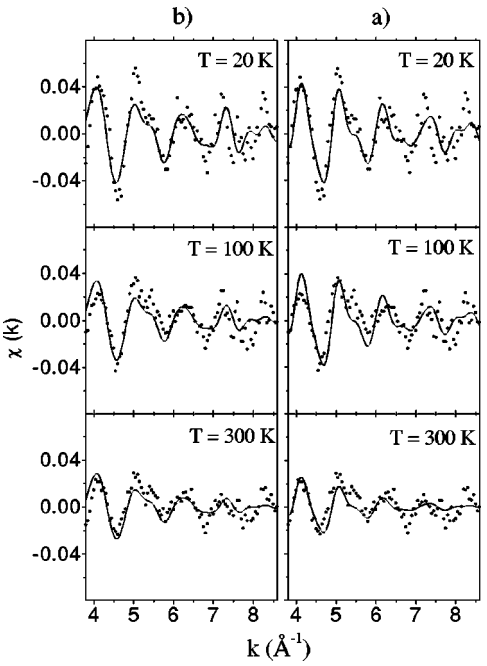

FIG. 6. Experimental EXAFS, $\chi(k)$, data for Na_8@Si-34 recorded at 20 K, 100 K, and 300 K compared to FEFF-FEFFIT simulation (continuous line) for a sodium displacement (a) $\Delta R=0.85$ Å and (b) $\Delta R=1$ Å. (a) and (b) Self-consistent and standard calculations, respectively (see text). The number of independent points is 15 and the fit parameters are the Debye temperature Θ_D, the reduced amplitude factor S_0^2, and the threshold energy E_0. For the self-consistent calculation, the fit parameters are $T=20$ K, $\Theta_D=386$ K, $E_0=-1$ eV, $S_0^2=1$; $T=100$ K, $\Theta_D=386$ K, $E_0=-1$ eV, $S_0^2=1$; and $T=300$ K, $\Theta_D=386$ K, $E_0=-1$ eV, $S_0^2=1$. For the standard calculation, the fit parameters are $T=20$ K, $\Theta_D=190$ K, $E_0=-1.2$ eV, $S_0^2=1$; $T=100$ K, $\Theta_D=260$ K, $E_0=-2$ eV, $S_0^2=1$; and $T=300$ K, $\Theta_D=400$ K, $E_0=-2$ eV, $S_0^2=1$.

the sodium atom with respect to the cage center was fixed to $\Delta R=0.85$ Å and $\Delta R=1$ Å for self-consistent scattering and overlapped atom potentials, respectively. We note that the amplitude of the signal is strongly affected by the temperature indicating a softening of the Debye temperature with respect on the one of the silicon host. In spite of the noise level, some high Fourier frequencies can be identified as characteristic of the clathrate lattice. The EXAFS fits are rather salient in the range $k=3.85$–7 Å^{-1}, where the signal is dominated by the contribution of the atoms belonging to the Si_{28} cage and become more tenuous at higher k. When using self-consistent calculations, the best fit is obtained with a single Debye temperature $\Theta_D=386$ K for the three experimental spectra, while standard overlapped potentials calculation needs a spread of Debye temperature [$\Theta_D=190$ K ($T=20$ K), $\Theta_D=260$ K ($T=100$ K), $\Theta_D=400$ K ($T=300$ K)]. One has to mention that such simulation might be significantly improved if we introduce a slight variation of the silicon-silicon distances (limited to 0.02 Å). We do not discuss this case since the physical meaning could be questioned owing to the increase of the number of fitting variables.

The reader may well ask about the confidence range of the sodium atom displacement determination. Figure 7 displays the comparison between experimental and calculated $\chi(k)$

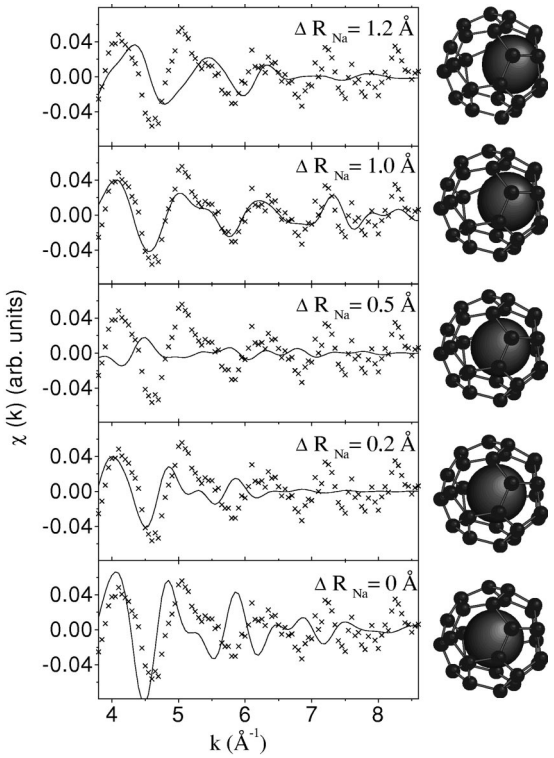

FIG. 7. Experimental EXAFS, $\chi(k)$, data for Na_8@Si-34 recorded at 20 K compared to FEFF-FEFFIT simulation (continuous line) for various sodium displacement $\Delta R=0$ Å, $\Delta R=0.2$ Å, $\Delta R=0.5$ Å, $\Delta R=1$ Å, $\Delta R=1.2$ Å. The fit parameters are $\Theta_D=190$ K, $E_0=-1.2$ eV, $S_0^2=1$. We have calculated XAFS spectrum from the standard overlapped atom potentials. We clearly observed a better fit for $\Delta R=1$ Å. The amplitude of the sodium displacement is shown in the right panel with the sodium radius equal to the atomic value.

for several values of the sodium displacement ($\Delta R=0$, $\Delta R=0.2$ Å, $\Delta R=0.5$ Å, $\Delta R=1$ Å, and $\Delta R=1.2$ Å) from the center of the Si cage towards the center of one of the hexagonal faces. We should note that the values $\Delta R=0$ and $\Delta R=0.2$ Å correspond to the expected structure derived from x-ray diffraction analysis and from calculations based on a Jahn-Teller deformation model, respectively.

We notice that the modeling of the data with displacement values of $\Delta R=0$, $\Delta R=0.2$ Å, $\Delta R=0.5$ Å, and $\Delta R=1.2$ Å gives rise to poor fits of the experimental data, even when allowing a large variation of the fitting parameters. We have also tried to optimize the sodium displacement ΔR for other directions of displacement (for instance, the sodium atom moves towards the center of a pentagon) but the fitting is always significantly poorer (Fig. 8). Figures 7 and 8 show that the best fit is obtained for a displacement towards the hexagon center of around $\Delta R=1$ Å and $\Delta R=0.85$ Å from overlapped atom potential and self-consistent calculations, respectively. From these curves, we estimate the value of ΔR to be 0.9 ± 0.2 Å.

In conclusion,[45] we have shown that sodium atoms are not located at the center of Si_{28} polyhedra in Na_8@Si-34 and that the experimental EXAFS signal can be perfectly simulated considering a sodium displacement of 0.9 ± 0.2 Å from the cage center towards the center of the hexagonal faces of the Si_{28} cages.

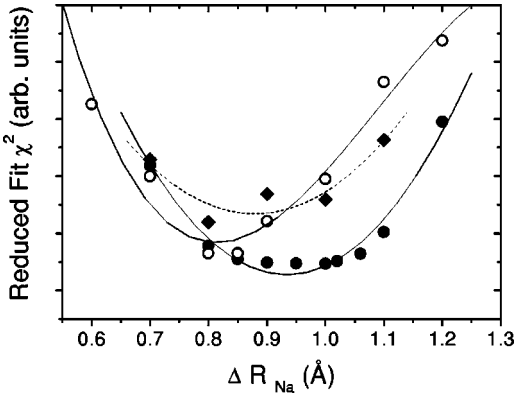

FIG. 8. Scaled measure of the goodness of fit parameter χ^2 for both SCF and standard calculations of the EXAFS signal. White circles display SCF calculations when the sodium atom moves towards the center of an hexagon. Dark circles (dark diamond, respectively) display the results using overlapped atom calculations when the sodium atom moves towards the center of a hexagon (pentagon, respectively). The best fits are obtained between $\Delta R=0.8$ Å and $\Delta R=1.1$ Å for the displacement towards the hexagons. We have to notice that χ^2 diverges when ΔR is lower than 0.5 Å and greater than 1.3 Å .

VI. DISCUSSION

A. Silicon state

Two effects are remarkable: the softening of the Si_{1s} energy in both clathrates with respect to the Si_{1s} energy in Si-2 and the energy shift between Na_1@Si-34 and Na_8@Si-34. Since the core level binding energy is a difference in total energy between the ground and excited states, it is useful to discuss the core level shift in terms of initial and final states. The so called initial state ''chemical effect'' is the modification of the electrostatic environment arising from the field of surrounding atoms or ions. The final state arises from the screening effect of the core hole by the surrounding atom cloud. Such a core hole is created during the photoelectron ejection. In most of the silicon compounds, the Si_{1s} core level line appears at higher energy than in Si-2 [1847 eV for Si-O, see Fig. 3(a)]. The low core level line energy observed in the nearly pure clathrate is consistent with earlier measurements performed on the valence band. It has been found that the Si_{3s} is shifted about 1.5 eV towards low energy in comparison with the Si_{3s} in Si-2. Owing to the screening of Si_{1s} core level by the electron outer shell, the total observed shift ($1843-1842.25=0.75\pm0.2$ eV) is lower than in $3s$ valence electron. Due to the insulating character in Na_1@Si-34, we are not able to precisely calculate the position of the Fermi level. In Na_8@Si-34, as mentioned above, the Si_{1s} shift can be understood as a partial filling of the bottom of the conduction band. The Fermi level will be located at 0.25 eV above the CBM. This value can be compared to the conduction-band energy dispersion near the Fermi level given by Smelyansky and Tse.[31] These authors calculated a separation of about 0.25 eV, which is consistent with our data.

B. Sodium state

Na_{1s} core level line in Na_8@Si-34 (1077.2 eV and 1077.8 eV related to the vacuum level by XPS and XAS spec-

troscopies, respectively) is just located above the values for the metallic state and beneath the atomic-state values. Such a value is not so far from the one observed in NaCl. However, we can rule out the possibility of having the sodium atom in an ionic state in the clathrate. In fact, Na_{1s} free ion state has the highest energy [1088.2 eV (Ref. 46), see Table II] since the core level shifts between the atom and free ion is mainly governed by an initial state contribution due to the $1s-3s$ Slater repulsion energy (8–9 eV).[42] On the contrary in alkali halide, the core level is lower than in the free ion owing to the Madelung contribution (around 9 eV), which counterbalances the $1s$-$3s$ Slater repulsion energy.[46] Since the silicon atoms are not ionized in the clathrate (there are sp^3 hybridized), the Madelung contribution must vanish in the clathrate. In addition, the Coulomb energy is weak since the distance between sodium and silicon atoms (about 4 Å) is greater than the one in NaCl (2.82 Å). Thus, the residual Madelung energy is not able to counterbalance the strong Slater energy. A sodium ionized state in the clathrate would be not too far from the free ion state (1088.2 eV), which is totally in disagreement with our experimental results. Consequently, the ionic state of Na in Na_8@Si-34 is not consistent with our results. This conclusion is in agreement with nuclear magnetic resonance spectroscopy.[18,47]

Now, let us examine the possibility of a metallic state. In sodium metal, the core level shift between the atom and the solid is mainly due to the final state. Using a self-consistent atom-jellium model, Lang and Williams[48] have shown that the core level shift of a sodium atom chemisorbed onto a pure jellium is about 4.5 eV for the final state and around -0.5 eV for the initial state. This explains roughly the shift between the atom and the solid (5.1 eV, see Table I). Since we found that the Na_{1s} in the clathrate is located above the metal-like [1074 eV (Ref. 49)] and beneath the atomiclike state [1079.1 eV (Ref. 49)], we can believe that the screening effect is less efficient than in the metal. This final state could be calculated following different ways. Since silicon atoms form a dielectric medium surrounding the sodium atom, we use the classical dielectric screening approach[50] to estimate the extra-atomic screening amplitude in the clathrate lattice. The charge in the screening cloud is $(1-1/\epsilon_0)e$, where ϵ_0 is the static dielectric constant and e the unit of charge. In the silicon, the charge cloud ($\epsilon_0=11.7$) is high enough to screen the core hole. An order of magnitude for the core level shift $\Delta E_{screening}$ is obtained from the Coulomb interaction leading to[50]

$$\Delta E_{screening}=\frac{1}{2}\left(1-\frac{1}{\epsilon_0}\right)\frac{e^2}{R}, \tag{1}$$

where R is a parameter that depends on the characteristic screening radius, the Thomas Fermi wave vector,[51] and the plasma frequency.

Such classical formula has been successfully applied to estimate the screening effect in most of the semiconductors and could be qualitatively extended to alkali metals where $\Delta E_{screening}$ diverges (i.e., $1/\epsilon_0=0$). For example, using the previous formula, the extrarelaxation energy is found at 7.5 eV and 5 eV for silicon and sodium, respectively. The strong relaxation energy in silicon is due to the high number of valence electrons ($n=4$) as compared to the alkaline metals ($n=1$).

Since in the clathrate case, R coincides with the Na-Si distance, the poor screening observed is probably due to the large distance between the sodium and the silicon atoms ($\sim$3.96 Å) (Ref. 52) as compared to the Na-Na distance in the metal (3.66 Å) and to the Si-Si distance in the clathrate lattice (about 2.38 Å). Our data validates a sodium state, which is intermediate between the atomlike (an insulator) and the metal-like behavior. We can estimate the relaxation for the sodium atom in the clathrate in the following way. A sodium atom in substitution inside a silicon network will be located at 2.35 Å from silicon neighbors while in the clathrate, it is located at a distance R not far away from the Si_{28} cage radius (3.95 Å). Let us adjust the formula first by a scaling law between the cage radius and the Si-Si distance (2.35 Å). This correction gives rise to a relaxation $\Delta E_{screening}$ of about 4.4 eV. Such a value should be compared to the experimental relaxation energy, which is the difference between the free atom and the clathrate core level lines ($1079.1-1077.2=1.9$ eV and $1079.1-1077.8=1.2$ eV for XPS and XAS, respectively). The model overestimates $\Delta E_{screening}$ since the screening of the sodium atom is lower than the one calculated for a silicon atom in the clathrate lattice.

C. Jahn-Teller and Peierls distortion

The more intriguing result of this work is the large displacement of the sodium atom inside the cage. Sodium atoms move away from the center of the Si_{28} cage of about 1 Å, which is considerably greater than the prediction of Demkov *et al.* (0.2 Å).[37] First, let us examine the implications of the sodium displacement on the site symmetry. Owing to the displacement in a direction perpendicular to the hexagon plane, the site symmetry was reduced from T_d to C_{3v}. This just coincides with the prediction of Demkov *et al.* who mention this new symmetry after the Jahn-Teller reconstruction. Nevertheless, these authors have calculated the Jahn-Teller distortion in Na_4@Si-34 where only half of the Si_{28} polyhedron are occupied by interstitial sodium. The alternance between empty and occupied cages changes the sodium lattice symmetry ($F4\bar{3}m$). However, in such a lattice, sodium atoms are totally isolated from each other and cannot form clusters. As mentioned previously each Si_{28} cage in Na_8@Si-34 is fully occupied by one sodium atom. Owing to the whole lattice symmetry, the sodium network forms a giant diamond lattice where each sodium atom has four neighbors ($d_{\text{Na-Na}}=6.34$ Å, when sodium atoms are in the center of the Si_{28} cages) (see Fig. 2). If the sodium atom moves away from the center of the cage, it appears as a dimerization as shown in Fig. 9. The formation of dimers can be explained by considering pairwise interactions. The strong interaction is probably spin-spin-type originated from an unpaired $3s$ electron in the cage. Thus, a partial covalent bonding in Na_2 will be responsible for an insulator state. In an earlier work, Hasegawa *et al.*[53] have mentioned a similar behavior in endohedral metallofullerenes $Y@C_{82}$. Using scanning tunneling microscopy, these authors have found that $Y@C_{82}$ molecules preferentially form a dimer. They have attributed this

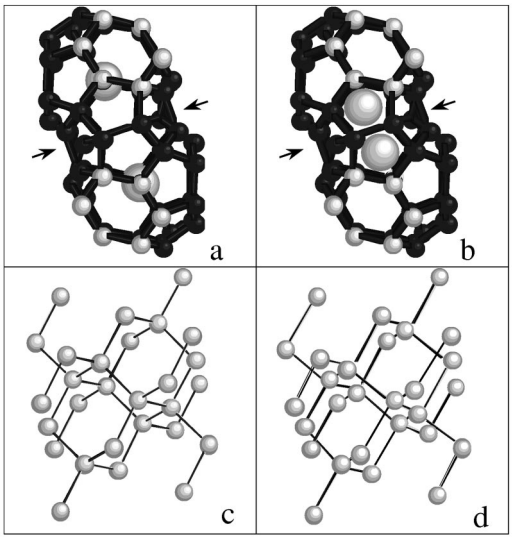

FIG. 9. Abutting Si_{28} cages with sodium located at (a) the center and (b) after Peierls distortion. The two Si_{28} cages share a hexagonal face (marked by arrows). (c) and (d) The sodium lattice before and after Peierls distortion, respectively. The sodium pairing form long chains.

dimerization to the spin-spin interaction. The sodium lattice symmetry breakdown presents some similarities with the Peierls transition.[54] Formally, the Peierls instability appears in one-dimensional metals and results from the competition between the elastic energy and the energy gain due to the appearance of an energy gap just at the Fermi level. In our case, the whole sodium lattice symmetry remains constant, involving dimer chains in the three-space direction. We notice that Peierls instability has been suggested in covalent[55] and lamellar structures.[56,57]

We expect that the gap is probably larger than the calculated Jahn-Teller gap since the spin-spin pairing localizes strongly the Na 3*s* electrons. In addition, the rigidity of the silicon network prevents any distortion of the network while C_{60} in doped pristine could be distorted by the Jahn-Teller effect. Thus, in the Na_8@Si-34 case the whole distortion is borne by sodium atoms. The Na-Na distance in the quasidimer is $(6.34-2\times1=4.34$ Å), which is much longer than the one of the free Na_2 dimer (3.08 Å). The relative increases of the Na-Na distance inside the clathrate with respect to the Na-Na distance in the free dimer, is attributed to the repulsion interaction involved in the sodium-silicon overlapping. Nevertheless, we can roughly estimate this bond length in an effective medium framework. The covalent bonding in free Na_2 is $1.63/a_H=3.08$ Å (Ref. 58), where a_H is the hydrogen radius. Assuming that the sodium lattice is ''dipped'' in a dielectric medium ϵ_{eff}, the equilibrium state of the quasidimer will be given just by scaling the hydrogen radius

$$a_{H\,eff}=a_H\epsilon_{eff} \tag{2}$$

and the Na-Na quasidimer distance

$$1.63/a_H=3.08\times\epsilon_{eff}\ \text{Å}\,. \tag{3}$$

The dielectric medium can be estimated from the comparison between the energy screening given by Eq. (1) and our experimental value deduced from XAS ($\Delta E_{screening}=1.2$ eV) and XPS ($\Delta E_{screening}=1.9$ eV), respectively,

$$\Delta E_{screening}=\frac{1}{2}\left(1-\frac{1}{\epsilon_{eff}}\right)\frac{e^2}{R}. \tag{4}$$

From these formula, we can deduce ϵ_{eff} and the distance of the quasidimer Na_2. We find $\epsilon_{eff}=1.7$, $\epsilon_{eff}=1.2$, and $d_{\text{Na-Na}}=5.24\pm0.8$ Å, $d_{\text{Na-Na}}=3.70\pm0.8$ Å, from XAS and XPS data, respectively. These rough estimations are not so far from the expected Na-Na distance in the quasidimer (4.34 Å). Nevertheless, we must keep in mind that this dielectric medium has not a real physical meaning but just introduces a qualitative interaction between sodium and the silicon host lattice.

VII. CONCLUSION

X-ray absorption spectroscopy performed on Na_8@Si-34 clathrate has shown a dimerization of the sodium atoms that can be assimilated to a Peierls distortion of the alkali lattice assisted by the Jahn-Teller effect, which is due to the combination of the true Jahn-Teller effect and the spin pairwise interactions. This dimerization is probably responsible for the nearly insulating state observed in Na_8@Si-34. The conduction mechanisms suggested by Demkov *et al.* who introduced the concept of Mott correlation induced metal seems a promising method and must be investigated theoretically. In such a way, this dimerization could be emphasized by quantum molecular dynamics effects especially for the particular case Na_8@Si-34. Moreover, an increase in the sodium concentration just above $x=8$ could destroy the Peierls gap owing to the $(F4\bar{3}m)$ symmetry breakdown and thus favor a metallic state. In addition, we have shown that the Fermi level is pulled up in the conduction band in Na_8@Si-34. Its position is in good agreement with first-principles calculations of Smelyansky and Tse.

[1] W. Kratschmer, L. D. Lamb, K. Fostiropoulos, and D. R. Huffman, Nature (London) **347**, 354 (1990).

[2] P. Byszewski, R. Diduszko, E. Kowalska, J. Fink-Finowicki, and A. Witowski, Appl. Phys. Lett. **61**, 2981 (1992).

[3] A. F. Hebard, M. J. Rosseinsky, R. C. Haddon, D. W. Murphy, S. H. Glarum, T. T. M. Palstra, A. P. Ramirez, and A. R. Kortan, Nature (London) **350**, 600 (1991).

[4] M. J. Rosseinsky, A. P. Ramirez, S. H. Glarum, D. W. Murphy, R. C. Haddon, A. F. Hebard, T. T. M. Palstra, A. R. Kortan, S. M. Zahurak, and A. V. Makhija, Phys. Rev. Lett. **66**, 2830 (1991).

[5] S. Iijima, Nature (London) **354**, 56 (1991).

[6] C. Cros and J. C. Bénéjat, Bull. Soc. Chim. Fr. **5**, 1739 (1972).

[7] C. Cros, M. Pouchard, and P. Hagenmuller, Solid State Chem. **2**, 570 (1970).

[8] J. S. Kasper, P. Hagenmuller, and M. Pouchard, Science **150**,

1713 (1965).
[9] E. Reny, M. Ménétrier, C. Cros, and M. Pouchard, C. R. Acad. Sci. Chim. France **1**, 129 (1998).
[10] K. E. Sim, Ph.D. thesis, Imperial College of Science and Technology, 1983.
[11] H. Kawaji, H.-O. Horie, S. Yamanaka, and M. Ishikawa, Phys. Rev. Lett. **74**, 1427 (1995).
[12] S. Yamanaka, H.-O. Horie, H. Kawaji, and M. Ishikawa, Eur. J. Solid State Inorg. Chem. **32**, 799 (1995).
[13] S. Yamanaka, H. O. Horie, N. Nakano, and M. Ishikawa, Fullerene Sci. Technol. **3**, 21 (1995).
[14] Y. Guyot, B. Champagnon, E. Reny, C. Cros, M. Pouchard, P. Mélinon, A. Perez, and I. Gregora, Phys. Rev. B **57**, R9475 (1998).
[15] P. Mélinon, P. Kéghélian, X. Blase, J. Le Brusc, A. Perez, E. Reny, C. Cros, and M. Pouchard, Phys. Rev. B **58**, 12 590 (1998).
[16] P. Mélinon, P. Kéghélian, A. Perez, B. Champagnon, Y. Guyot, L. Saviot, E. Reny, C. Cros, and M. Pouchard, Phys. Rev. B **59**, 10 099 (1999).
[17] S. L. Fang, L. Grigorian, P. C. Eklund, G. Dresselhaus, M. S. Dresselhaus, H. Kawaji, and S. Yamanaka, Phys. Rev. B **57**, 7686 (1998).
[18] J. Gryko and P. F. McMillan, Phys. Rev. B **54**, 3037 (1996).
[19] J. Dong, O. F. Sankey, and J. Kern, Phys. Rev. B **60**, 950 (1999).
[20] N. F. Mott, Solid State Chem. **6**, 348 (1973).
[21] E. Kaxiras, L. M. Zeger, A. Antonelli, and Y. M. Juan, Phys. Rev. B **49**, 8446 (1994).
[22] D. M. Bylander and L. Kleinman, Phys. Rev. B **47**, 10 967 (1993).
[23] L. M. Zeger, Yu-Min Juan, E. Kaxiras, and A. Antonelli, Phys. Rev. B **52**, 2125 (1995).
[24] J. Kim, G. Galli, J. W. Wilikins, and A. Canning, J. Chem. Phys. **108**, 2631 (1998).
[25] A. A. Demkov, W. Windl, and O. F. Sankey, Phys. Rev. B **53**, 11 288 (1996).
[26] G. B. Adams, M. O. Keefe, A. A. Demkov, O. F. Sankey, and Y. M. Huang, Phys. Rev. B **49**, 8048 (1994).
[27] S. Saito and A. Oshiyama, Phys. Rev. B **51**, 2628 (1995).
[28] M. O. Keefe, G. B. Adams, and O. F. Sankey, Phys. Rev. Lett. **68**, 2325 (1992).
[29] M. Menon, E. Richter, and K. R. Subbaswamy, Phys. Rev. B **56**, 12 290 (1997).
[30] D. Kahn and J. P. Lu, Phys. Rev. B **56**, 13 898 (1997).
[31] V. I. Smelyansky and J. S. Tse, Chem. Phys. Lett. **264**, 459 (1997).
[32] Y. N. Xu, M. Z. Huang, and W. Y. Ching, Phys. Rev. B **46**, 4241 (1992).
[33] O. Gunnarsson, S. Satpathy, O. Jepsen, and O. K. Andersen, Phys. Rev. Lett. **67**, 3002 (1991).
[34] M. Schlüter, M. Lannoo, M. Needels, G. A. Baraff, and D. Tomanek, Phys. Rev. Lett. **68**, 526 (1992).
[35] M. Lannoo, G. A. Baraff, and M. Schlüter, Phys. Rev. B **44**, 12 106 (1992).
[36] G. B. Adams, O. F. Sankey, J. B. Page, and M. O. Keefe, Chem. Phys. **176**, 61 (1993).
[37] A. A. Demkov, O. F. Sankey, K. E. Schmidt, G. B. Adams, and M. O. Keefe, Phys. Rev. B **50**, 17 001 (1994).
[38] F. Brunet, P. Mélinon, P. Kéghélian, A. Perez, A. M. Flank, P. Lagarde, E. Reny, C. Cros, and M. Pouchard (unpublished).
[39] In XAS, the calibration was related to the zinc L_{III} core level fixed in ZnS at 1021.8 eV (to the CBM). In fact, we discuss in both spectroscopies (XPS and XAS) the relative energy difference between the sodium state in NaCl and clathrate. Of course, the calibration was the same for all the samples.
[40] K. Siegbahn, C. Nordling, A. Fahlman, R. Nordberg, K. Hamrin, J. Hedman, G. Johansson, T. Berymark, S. E. Karlsson, I. Lindgren, and B. J. Lindberg, Nova Acta Regiae Soc. Sci. **20**, 1 (1967).
[41] This assumption is rather adapted in the case of quantum confinement in silicon superlattices [see Z. H. Lu, D. J. Lockwood, and J. M. Baribeau, Nature (London) **378**, 258 (1995)]. We assume that the gap opening in the clathrate could be looked at as a confinement effect in the cages which have a symmetry different from the whole lattice.
[42] W. F. Egelhoff, Surf. Sci. Rep. **6**, 253 (1987).
[43] A. L. Ankudinov, B. Ravel, J. J. Rehr, and S. D. Conradson, Phys. Rev. B **68**, 7565 (1998).
[44] M. Newille, B. Ravel, D. H. Askel, J. J. Rehr, E. A. Stern, and Y. Yacbi, Physica B **154**, 208 (1995).
[45] Tabulated McKale [A. G. McKale, G. S. Knapp, and S. K. Chan, Phys. Rev. B **33**, 841 (1986)] phase and amplitude files and experimental phase and amplitude extracted from NaCl were also used. This simple model gives rise to a displacement of about 1 Å in agreement with *ab initio* calculations.
[46] P. H. Citrin and T. Darrah Thomas, J. Chem. Phys. **57**, 4446 (1972).
[47] G. K. Ramachandran, P. McMillan, J. Diefenbacher, J. Gryko, J. Dong, and O. F. Sankey, Phys. Rev. B **60**, 12 294 (1999), and references therein.
[48] N. D. Lang and A. R. Williams, Phys. Rev. B **16**, 2408 (1977).
[49] M. S. Banna, B. Wallbank, D. C. Frost, A. M. McDowell, and J. S. H. Q. Perera, J. Chem. Phys. **68**, 5459 (1978).
[50] F. Bechstedt, Phys. Status Solidi B **112**, 9 (1982), and references therein.
[51] P. Csavinszky, Phys. Rev. B **28**, 6076 (1983).
[52] In fact, we have found that sodium is not located at the center of the cage. Thus, we have a spread of the R values. Our model being only qualitative, we take the mean value, which is close to the initial cage radius.
[53] Y. Hasegawa, Y. Ling, S. Yamazaki, T. Hashizume, H. Shinohara, and T. Sakurai, Mater. Sci. Eng., A **217/218**, 23 (1996).
[54] N. F. Mott and E. A. Davis, *Electronic Processes in Noncrystalline Materials* (Clarendon Press, Oxford, 1971).
[55] J. P. Gaspard, F. Marinelli, and A. Pellegatti, Europhys. Lett. **3**, 1095 (1987).
[56] A. San Miguel, M. Gauthier, J. P. Itié, A. Polian, H. Libotte, and J. P. Gaspard (unpublished).
[57] The dimerization process is well described from the Hubbard Hamiltonian framework. It appears when the electron-electron correlation (U) is large enough with respect to the hopping integral β. It is easy to check that a low coordinated system (N) favors the dimerization. The Peierls transition is a limit case where $N=2$. In our case, the coordinance number is $N=4$ lower than in the bulk phase (N about 12). At a first level, the correlation is given by the atomic ionization potential minus the electron affinity (about 5 eV) [J. Friedel, in *Microclusters*, edited by S. Sugano, Y. Nishini, and S. Ohnishi (Springer-Verlag, Berlin, 1986)]. Such a value is still overestimated. We can estimate the ($3s$) bandwidth from our experimental data. This band corresponds roughly to the Fermi level minus the CBM (0.25 eV). Owing to the simplicity of the Hubbard model one finds that the

system is strongly dimerized ($U/\beta \gg 1$) for Na_x@Si-34, $x=8$. This is not in agreement with experiments that show a metal-like behavior above $x=8$. Indeed, the correlation can be estimated (Demkov *et al.*, Ref. 38) by the Coulomb self-interaction of a uniformly charged sphere of radius $R=5$ Å (the extent of the Na 3*s* wave function). The value is lower (1.7 eV) but does not explain the insulator-to-metal transition for $x>8$. Indeed the classical jellium approach is interesting since the Coulomb interaction introduces the dielectric constant. Since the sodium metal is surrounded by a dielectric medium, the screening due to the silicon electron cloud must pull down the correlation energy as far as the dimerization vanishes for $x>8$.

[58] G. Herzberg, *Spectra of Diatomic Molecules* (Van Nostrand, New York, 1950).